Supplementary Information

All-Selenolate-Protected Eight-Electron Platinum/Silver Nanoclusters

Tzu-Hao Chiu,[a] Jian-Hong Liao,[a] Franck Gam,[b] Isaac Chantrenne,[b] Samia Kahlal,[b] Jean-Yves Saillard,*[b] and C. W. Liu*[a]

[a] Department of Chemistry, National Dong Hwa University, Hualien 974301, Taiwan (R.O.C.)
E-mail: chenwei@mail.ndhu.edu.tw; http://faculty.ndhu.edu.tw/~cwl/index.htm
[b] Univ. Rennes, CNRS, ISCR-UMR 6226, Rennes F-35000, France

Experimental Section.

1.1 General remarks

All chemicals were purchased from commercial sources and used as received. Solvents were purified following standard protocols.[1] All reactions were performed in oven-dried Schlenk glassware using standard inert atmosphere techniques. All reactions were carried out under N_2 atmosphere by using standard Schlenk techniques. $[PtAg_{20}\{S_2P(O^nPr)_2\}_{12}]$,[2] $(NH_4)[Se_2P(OR)_2]$ (R = ^nPr, **1a**; ^iPr, **1b**)[3] and $(NH_4)[Se_2P(CH_2CH_2Ph)_2]$[4] were prepared by a slightly modified procedure reported earlier literature. ESI-mass spectrum recorded on a Fison Quattro Bio-Q (Fisons Instruments, VG Biotech, U. K.). NMR spectra were recorded on a Bruker Avance II 400.13 MHz NMR spectrometer that operates at 400.13 MHz while recording ^1H, at 161.9 MHz for ^{31}P NMR. The chemical shift (δ) and coupling constant (J) are reported in ppm and Hz, respectively. Residual solvent protons were used as a reference (δ, ppm, CDCl$_3$, 7.26). $^{31}P\{^1H\}$ NMR spectra were referenced to external 85% H_3PO_4 at δ 0.00. UV-visible absorption spectra were measured on a Perkin Elmer Lambda 750 spectrophotometer using quartz cells with path length of 1 cm. Luminescence spectra and lifetime were recorded on an Edinburgh FLS920 fluorescence spectrometer. X-ray photoelectron spectroscopy (XPS) spectra were recorded on a spectrometer (VG Multilab 2000-Thermo Scientific Inc. UK, Kα) with a microfocus monochromated Al Kα X-ray working with high photonic energies from 0.2 to 3 KeV.

1.2 synthesis

1.2.1 $[PtAg_{20}\{Se_2P(O^nPr)_2\}_{12}]$, 1a

In a Flame-dried Schlenk, $[PtAg_{20}\{S_2P(O^nPr)_2\}_{12}]$ (0.02 g, 0.004 mmol), was dissolved in THF (5 mL) with twelve equivalents of $NH_4[Se_2P(O^nPr)_2]$ (0.016 g, 0.048 mmol) and the resulting mixture was stirred at 0°C less than 1 minute. The solvent was evaporated under vacuum and residue was pure by hexane to remove the

$NH_4[S_2P(O^nPr)_2]$ ligand. Lastly, the hexane was evaporated under vacuum to get a pure dark orange powder with composition $[PtAg_{20}\{Se_2P(O^nPr)_2\}_{12}]$ (Yield: 0.02 g, 85%, based on Ag). $^{31}P\{^1H\}$ NMR (161.97 MHz, CDCl$_3$, δ, ppm): 74.1 ($^1J_{PSe}$ = 609, 709 Hz). ^1H NMR (400.13 MHz, CDCl$_3$, δ, ppm): 0.99 (t, 72H, *CH$_3$*), 1.72-1.83 (m, 48H, *CH$_2$*), 4.01-4.16 (m, 48H, O*CH$_2$*). ESI-MS (m/z): exp. 6145.3 (calc. for $[1a + Ag^+]^+$: 6145.1). UV-vis [λ$_{max}$ in nm, (εin M^{-1}cm^{-1})] 388 (35600), 466 (25600). Elem. Anal for $(PtAg_{20}Se_{24}P_{12}O_{24}C_{72}H_{168})\cdot2(C_6H_{14})$: (calc. C% 16.25; H% 3.18). Found: C% 16.85; H% 3.14

1.2.2 $[PtAg_{20}\{Se_2P(O^iPr)_2\}_{12}]$, 1b

The synthetic procedure was similar to **1a**, $NH_4[Se_2P(O^iPr)_2]$ was used instead of $NH_4[Se_2P(O^nPr)_2]$. (Yield: 0.018 g, 75%, based on Ag) $^{31}P\{^1H\}$ NMR (161.97 MHz, CDCl$_3$, δ, ppm): 67.3 ($^1J_{PSe}$ = 597, 711 Hz). ^1H NMR (400.13 MHz, CDCl$_3$, δ, ppm): 1.34-1.38 (m, 144H, *CH$_3$*), 4.86-4.96 (m, 24H, O*CH*). ESI-MS (m/z): exp. 6145.3 (calc. for $[1b + Ag^+]^+$: 6145.1). UV-vis [λ$_{max}$ in nm, (εin M^{-1}cm^{-1})] 391 (35900), 470 (28700). Elem. Anal for $PtAg_{20}Se_{24}P_{12}O_{24}C_{72}H_{168}$: (calc. C% 14.32; H% 2.8). Found: C% 13.91; H% 2.98

1.2.3 $[PtAg_{20}\{Se_2P(CH_2CH_2Ph)_2\}_{12}]$, 2

$PtAg_{20}\{S_2P(O^nPr)_2\}_{12}$ (0.02 g, 0.004 mmol) was dissolved in THF (30 mL) at -20°C under N$_2$. $NH_4[Se_2P(CH_2CH_2Ph)_2]$ (0.02 g, 0.048 mmol) was then added and kept stirring 5 minutes. The solution was dried under vacuum to get red solid. It passed through an alumina column which a 2:8 mix of acetone and *n*-hexane was used as the elution solvent. The last red eluent was collected and dried to yield $[PtAg_{20}\{Se_2P(CH_2CH_2Ph)_2\}_{12}]$ (Yield: 0.018 g, 62%, based on Ag). $^{31}P\{^1H\}$ NMR (161.97 MHz, CDCl$_3$, δ, ppm): 31.9 ($^1J_{PSe}$ = 454 Hz, 554 Hz). ^1H NMR (400.13 MHz, CDCl$_3$, δ, ppm): 2.69 -3.05 (m, 96H, *CH$_2$CH$_2$*), 6.98-7.18 (m, 120H, *-Ph*). ESI-MS (m/z): 3625.6 (calc. for $[2 + Ag^+ + H^+]^{2+}$: 3626.7). UV-vis [λ, nm (ε, M^{-1} cm^{-1})]: 414 (36000), 484 (31700). Elem. Anal for $(PtAg_{20}Se_{24}P_{12}C_{204}H_{244})\cdot2(C_6H_{14})$: (calc. C% 33.49; H% 3.36). Found: C% 33.17; H% 3.32

1.3 X-ray crystallography

Single crystals suitable for X-ray diffraction analysis of **1a**, **1b** and **2** were obtained by diffusing hexane into concentrated acetone solution at 4°C within a week. The single crystals were mounted on the tip of glass fiber coated in paratone oil, then frozen. Data were collected on a Bruker APEX II CCD diffractometer using graphite monochromated Mo Kα radiation (λ = 0.71073 Å) at 150 (**1a, 2**) and 100 K (**1b**). Absorption corrections for area detector were performed with SADABS[5] and the

integration of raw data frame was performed with SAINT.[6] The structure was solved by direct methods and refined by least-squares against F^2 using the SHELXL-2018/3 package,[7] incorporated in SHELXTL/PC V6.14.[8] All non-hydrogen atoms were refined anisotropically. CCDC 1985876 (**1a**), 2069764 (**1b**) and 2069767 (**2**) contains the supplementary crystallo-graphic data for compounds **1**–**2** in this article. These data can be obtained free of charge from The Cambridge Crystallographic Data Centre via www.ccdc.cam.ac.uk/data_request/cif.

1.4 Computational details

Geometry optimization were carried out at the density functional theory (DFT) level using the Gaussian16 package[9] on the simplified models **1'** and **3'**. The BP86 functional[10] was used together with the general triple-ζ -polarized Def2-TZVP basis set from EMSL Basis Set Exchange Library.[11] The optimized geometries were characterized as true minima by vibrational analysis. The natural atomic orbital (NAO) charges were computed with the NBO6.0 program[12] on single-point calculations performed with the BP86 functional and the LANL2DZ basis set for computational limitation.[13] The UV-visible transitions were calculated by means of time-dependent DFT (TD-DFT) calculations, with the CAM-B3LYP functional[14] and the Def2-TZVP basis set. The UV-visible and CD spectra were simulated from the computed TD-DFT transitions and their oscillator strengths by using the SWizard program,[15] each transition is associated with a Gaussian function of half-height width equal to 2000 cm^{-1}. The compositions of the molecular orbitals were calculated using the AOMix program.[16]
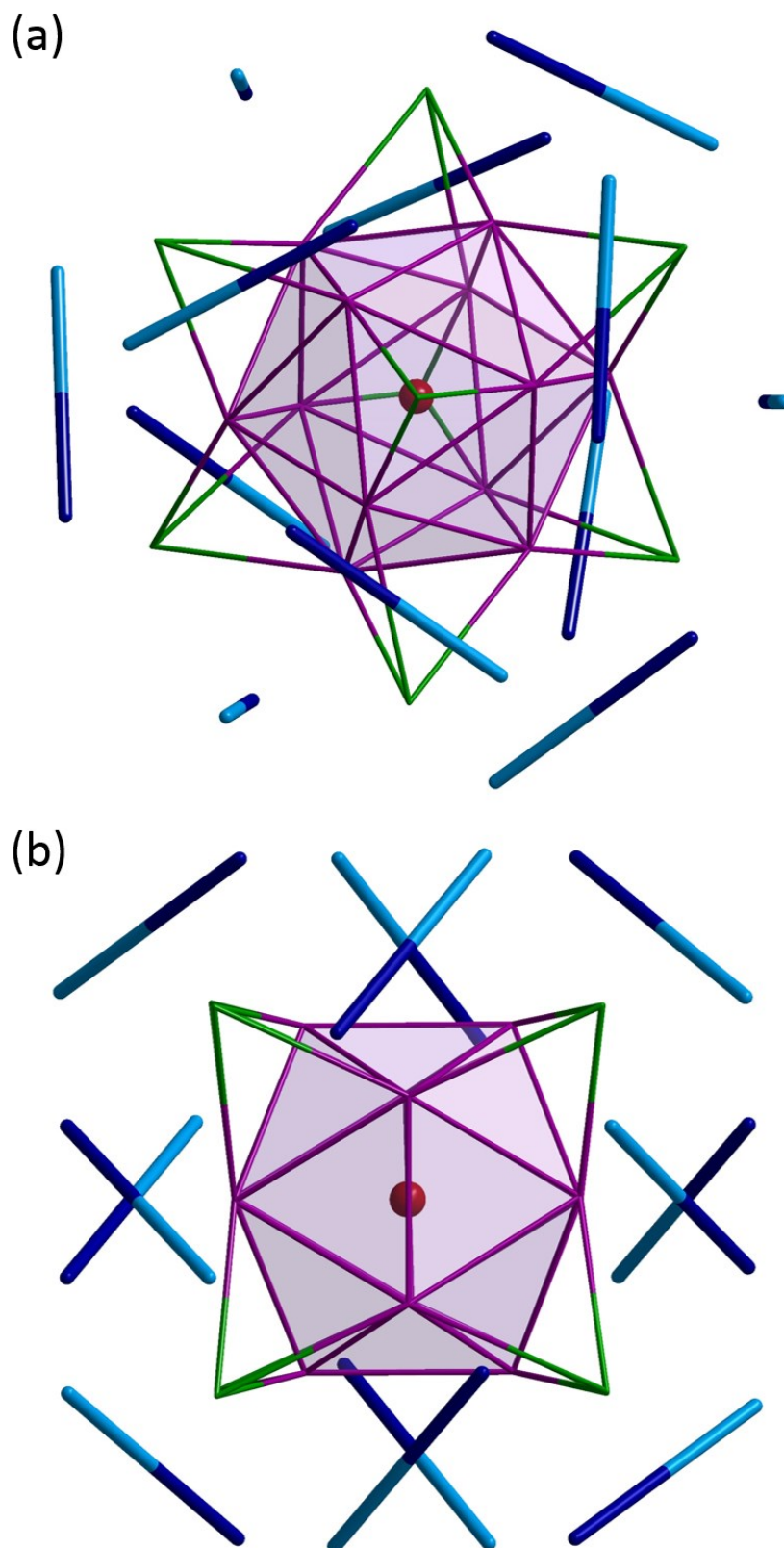
Figure S1. (a) A schematic representation of $PtAg_{20}(dsep/dsepi)_{20}$ which is viewed from C_3 axis and (b) C_2 axis, respectively. The ligands were drew as blue-cyan sticks, which is the connection of Se...Se of dsep/dsepi ligands. The blue side on the stick represents the Se connects to two Ag atoms, and the cyan side connect to one Ag atom.
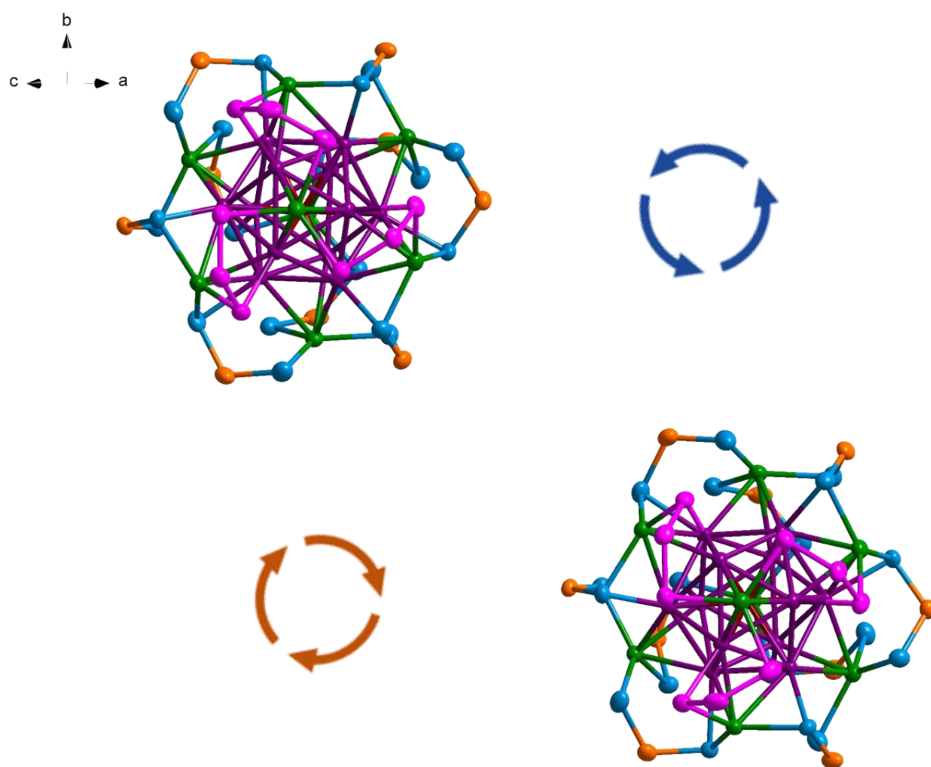
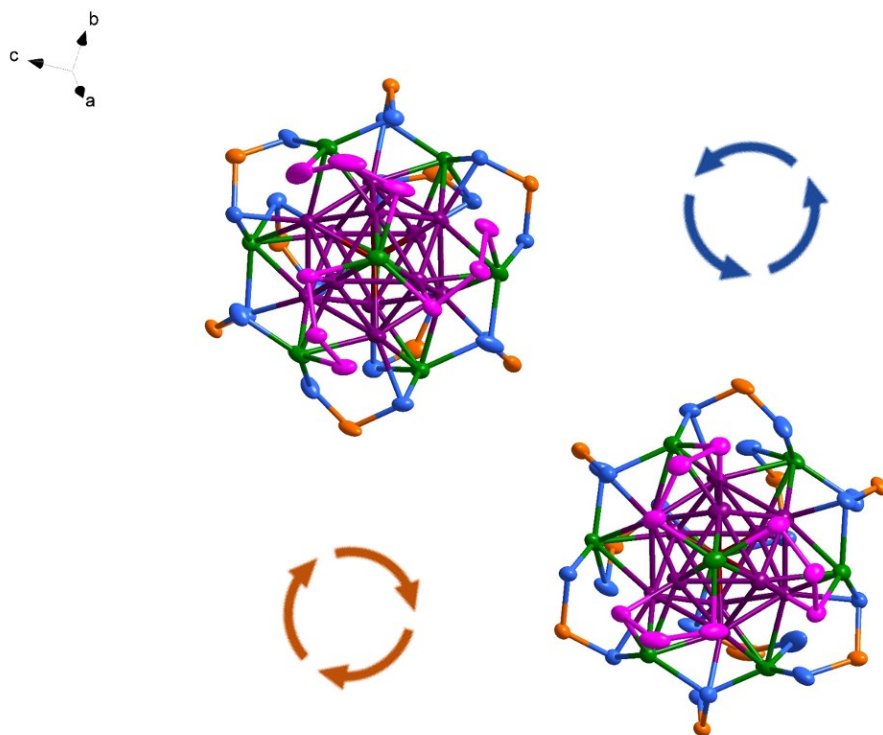**Figure S2.** Packing diagram of **1b** shows two enantiomers.
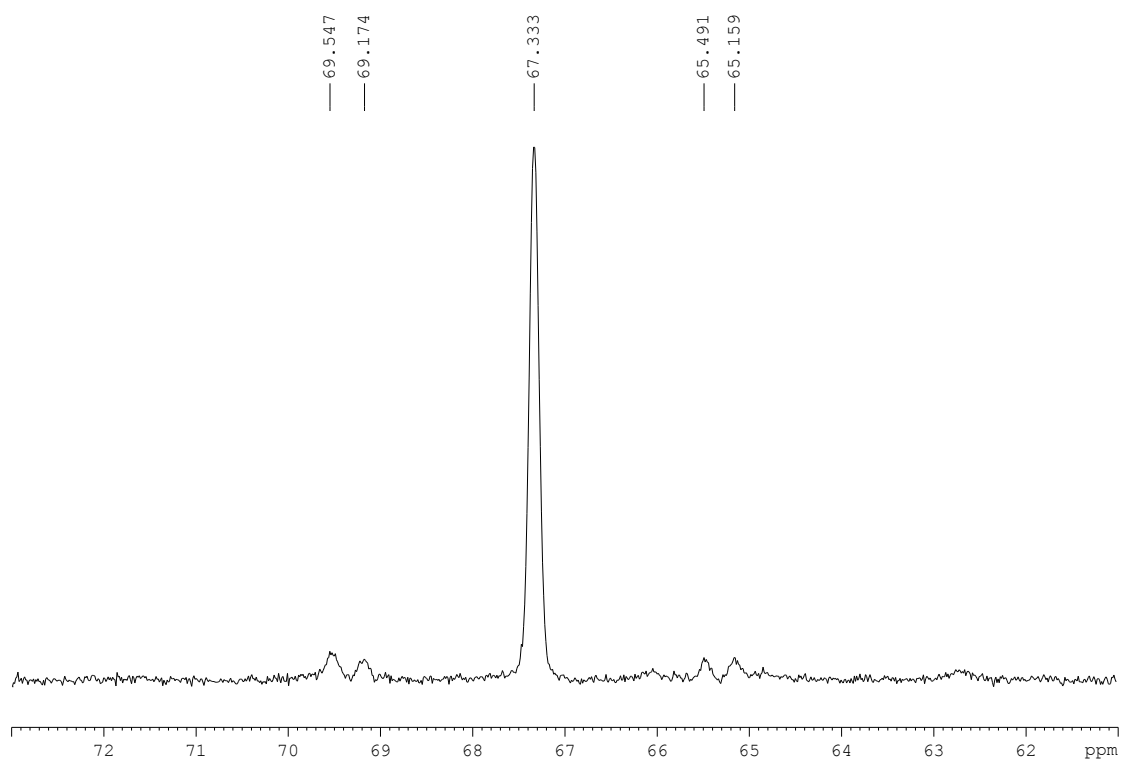

Figure S3. Packing diagram of **2** shows two enantiomers.

Figure S4. ^{31}P{^{1}H} NMR spectrum of **1b**.
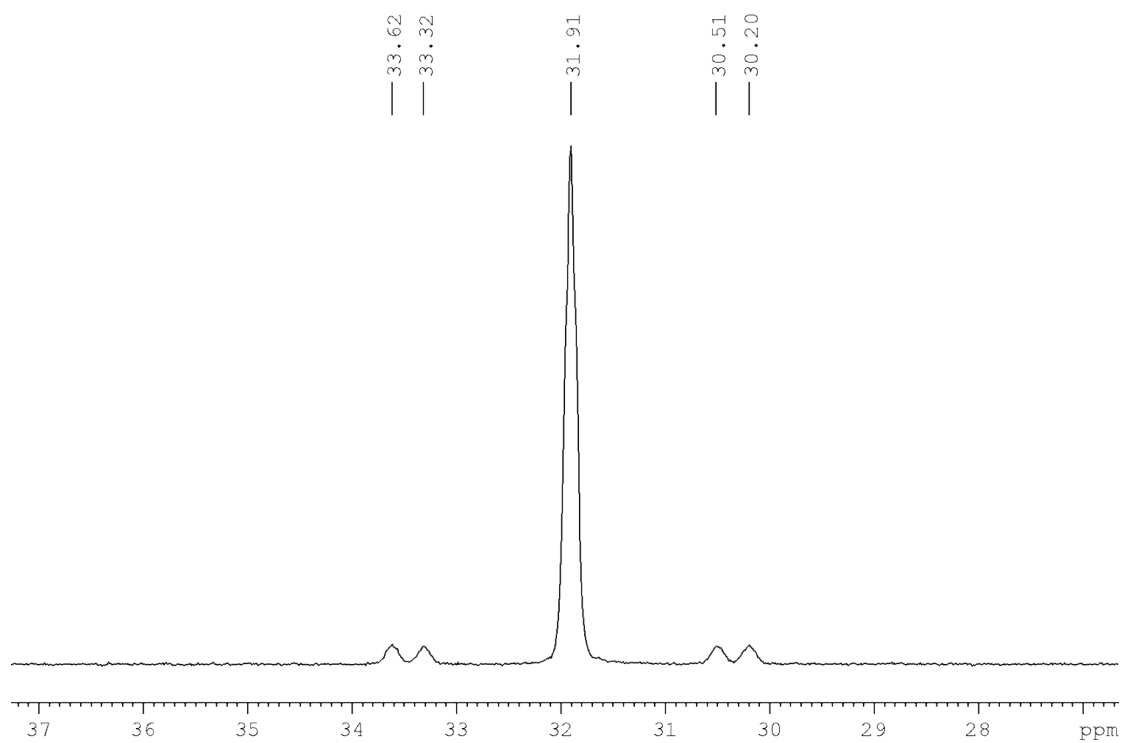
Figure S5. ^{31}P{^{1}H} NMR spectrum of **2**.
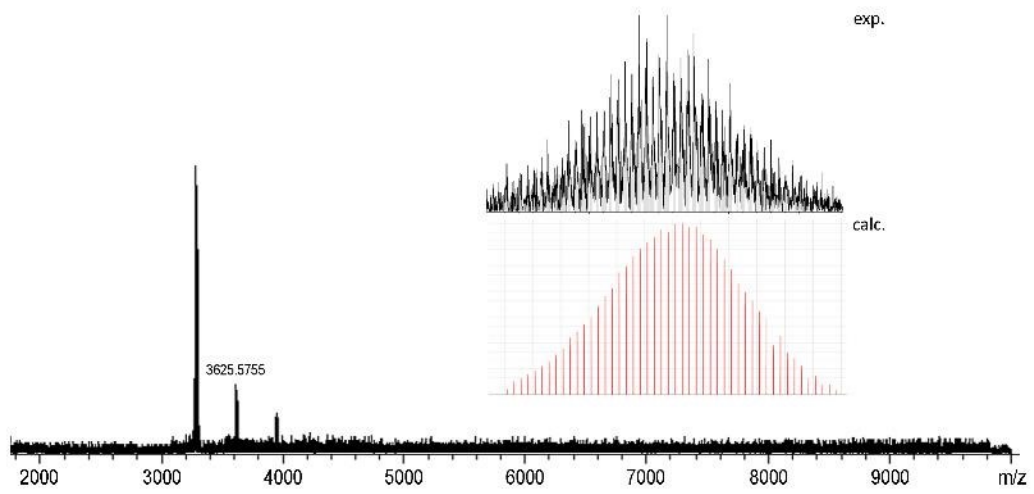
Figure S6. Positive-mode ESI-MS of **2**.
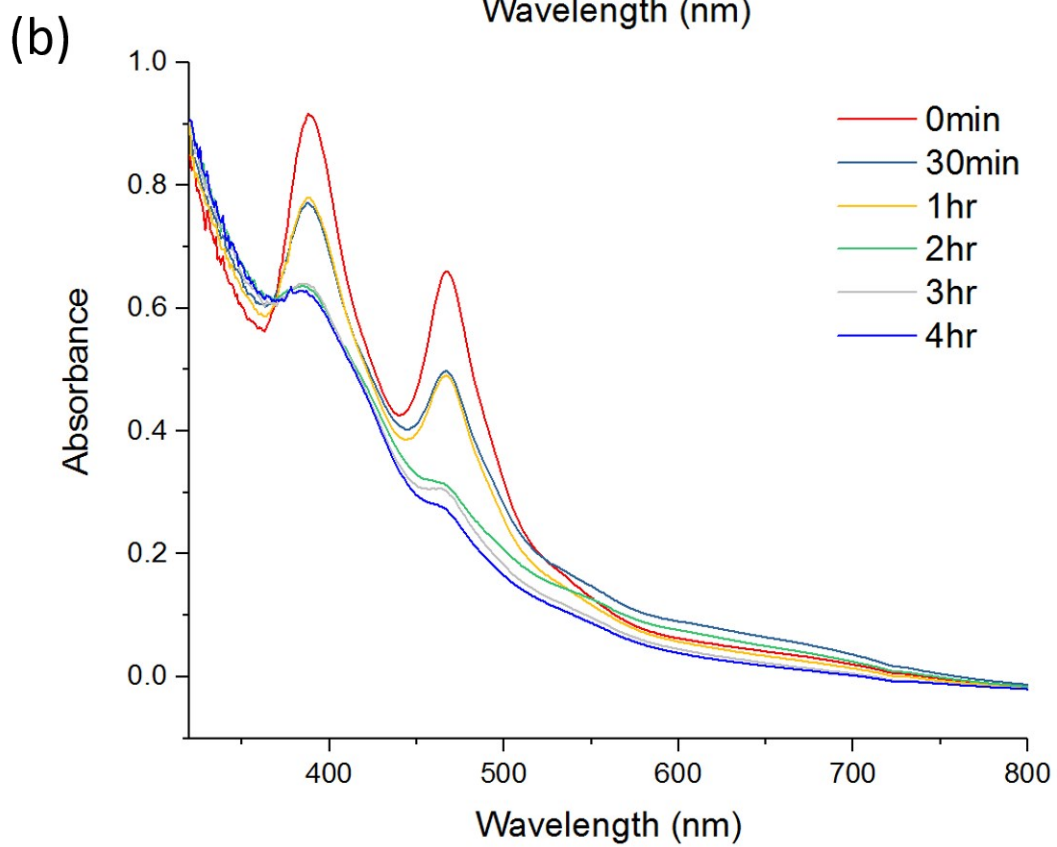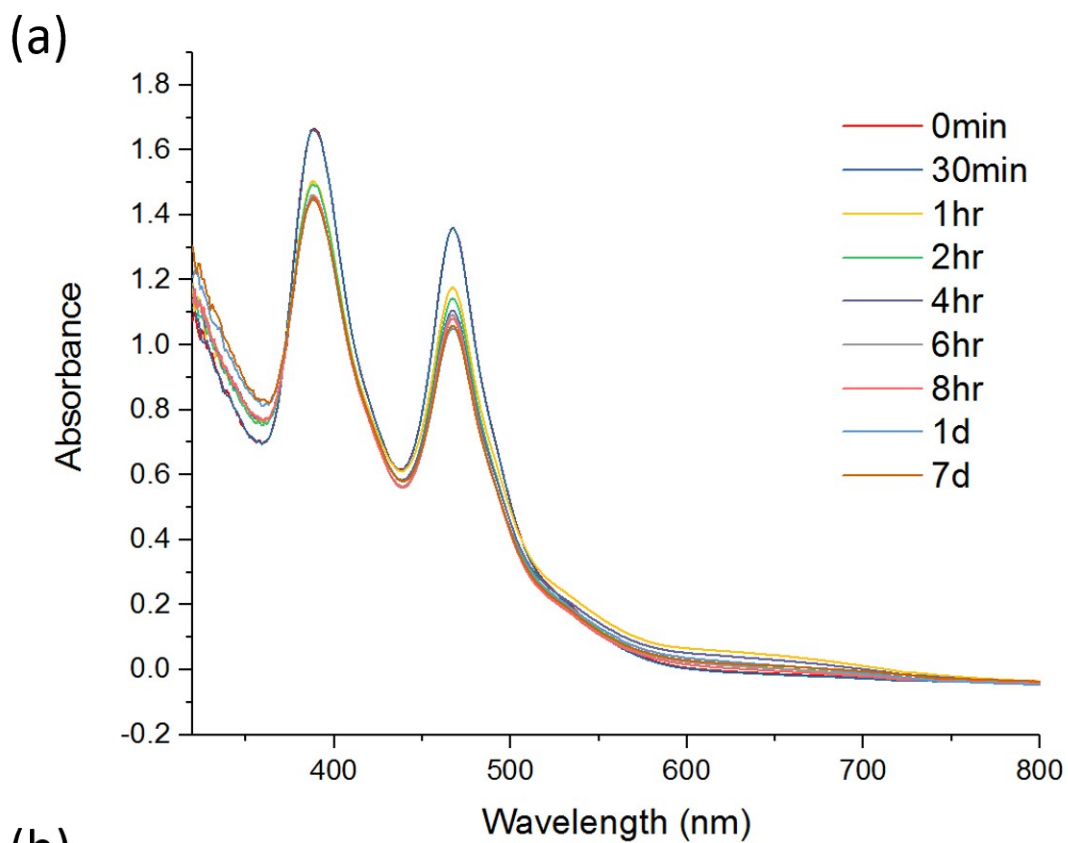
Figure S7. Time-dependent absorption spectrum of **1a** (a) in dark and (b) under light.
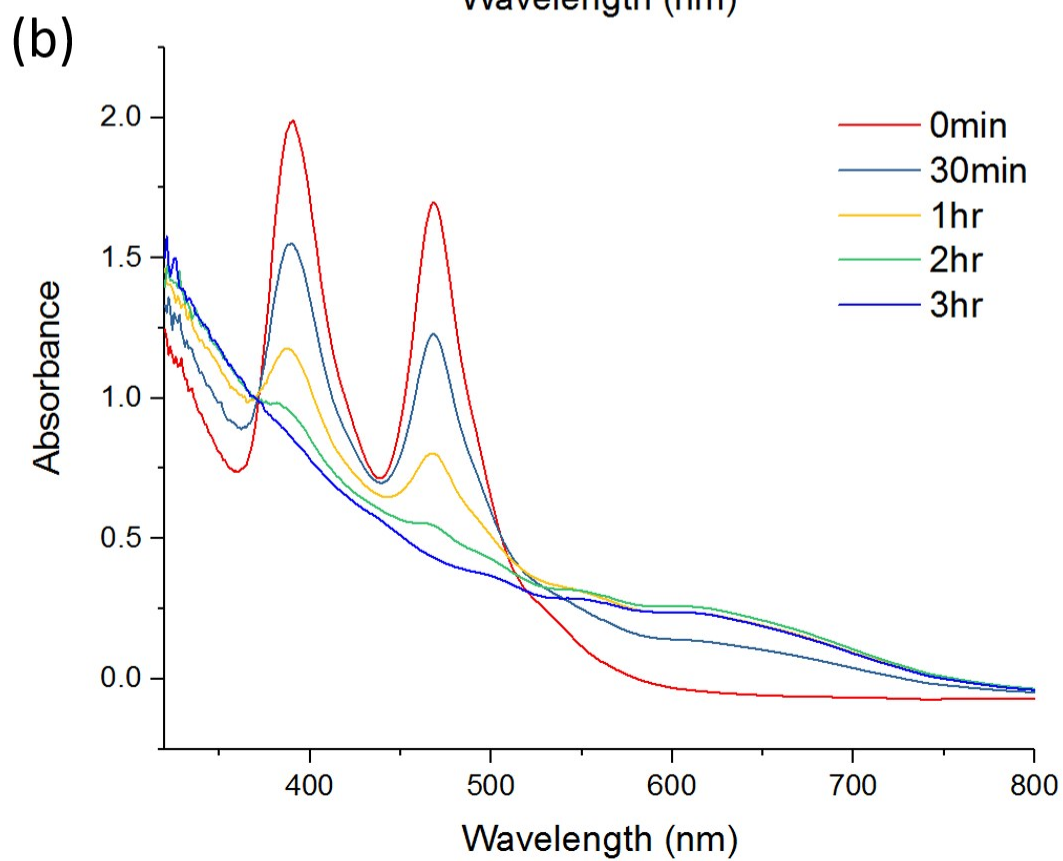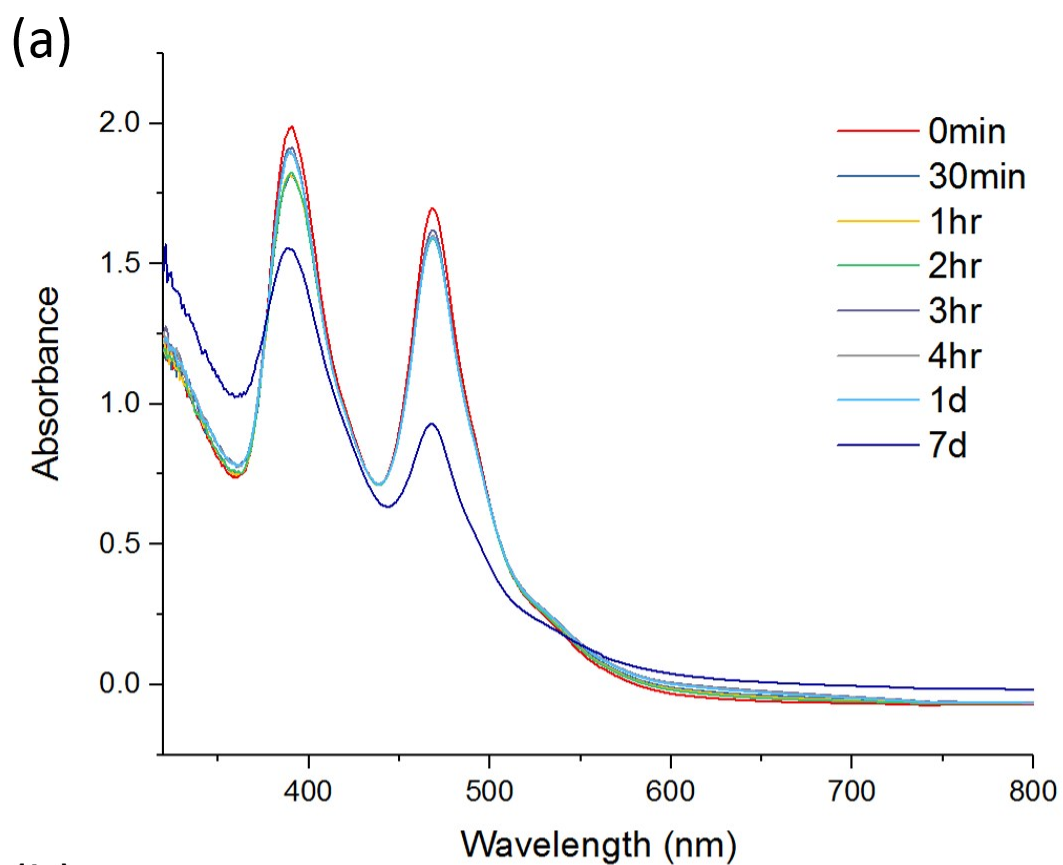
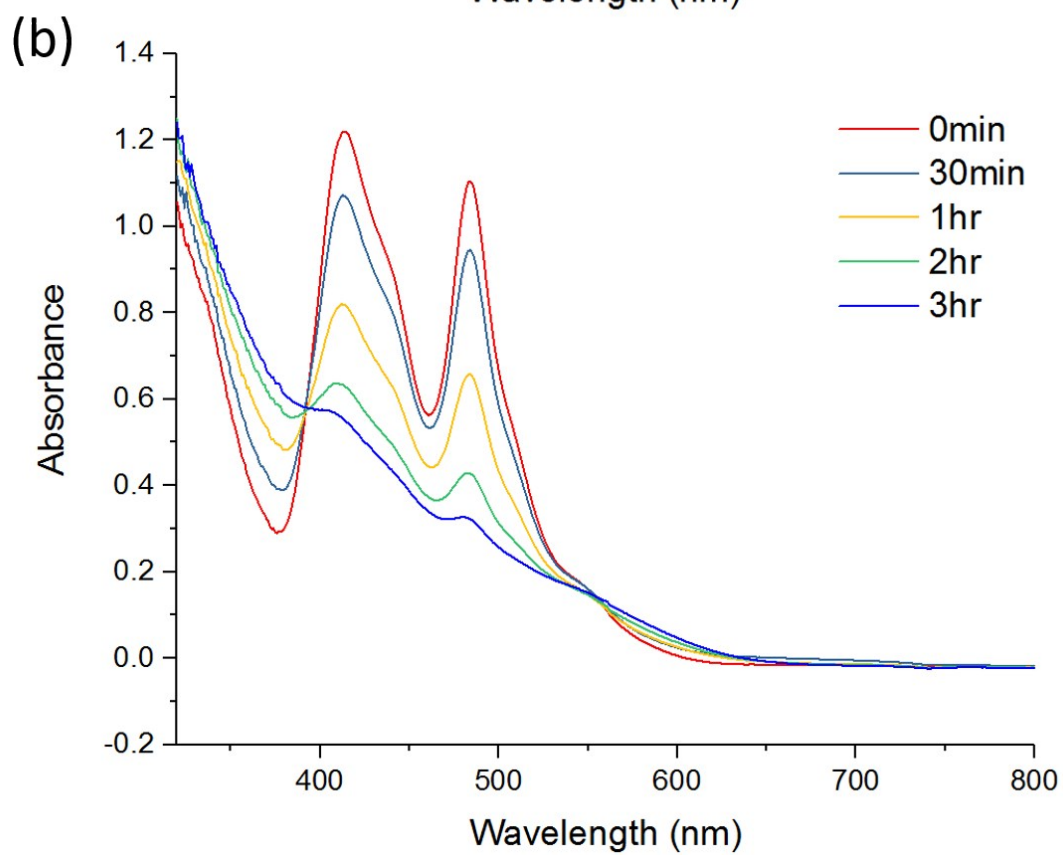**Figure S8.** Time-dependent absorption spectrum of **1b** (a) in dark and (b) under light.
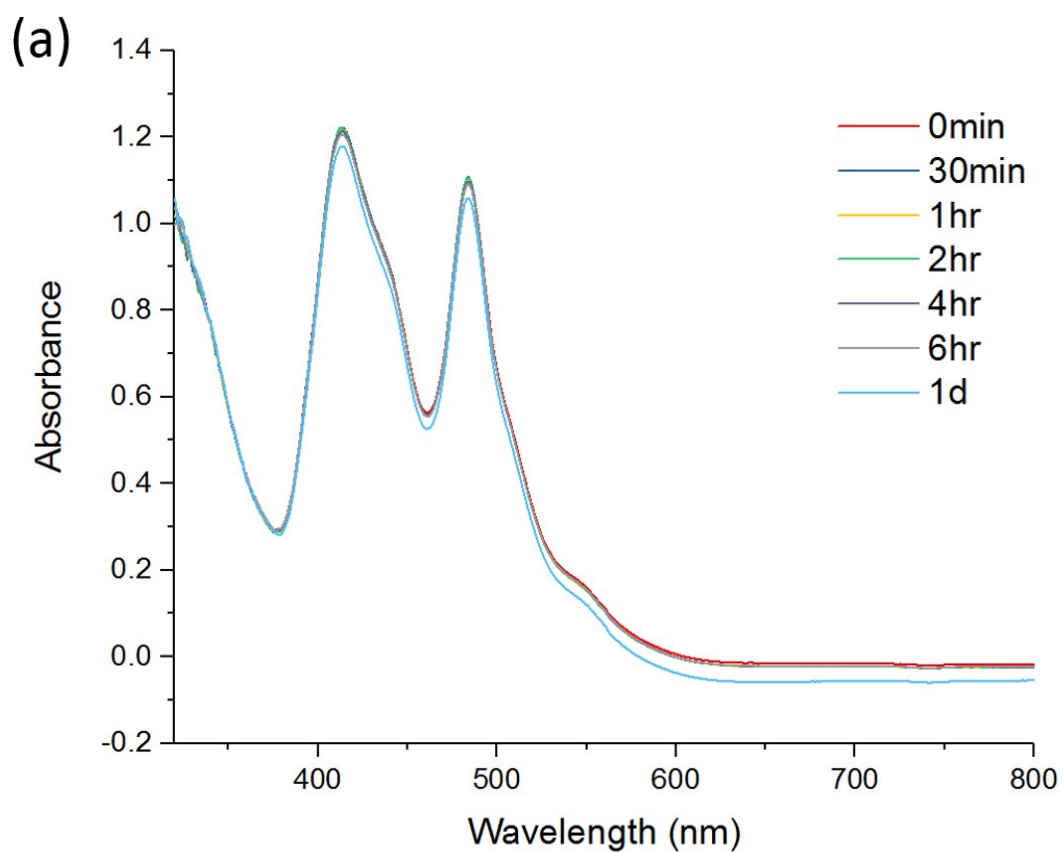
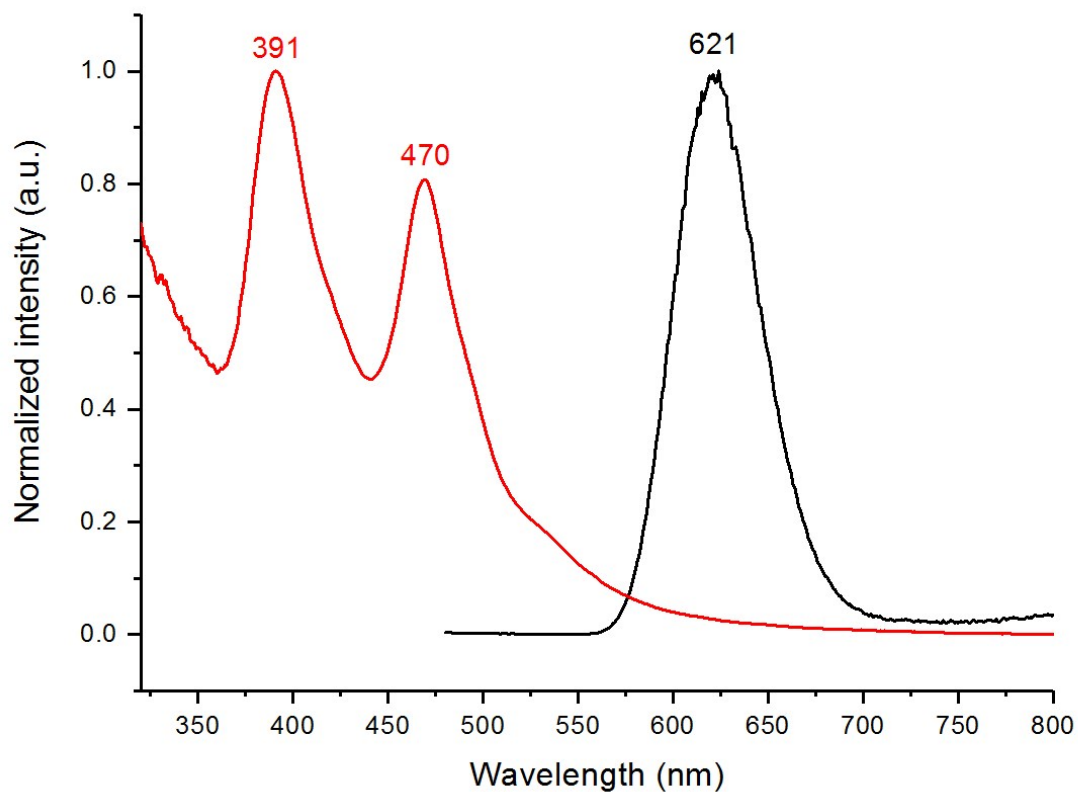**Figure S9.** Time-dependent absorption spectrum of **2** (a) in dark and (b) under light.

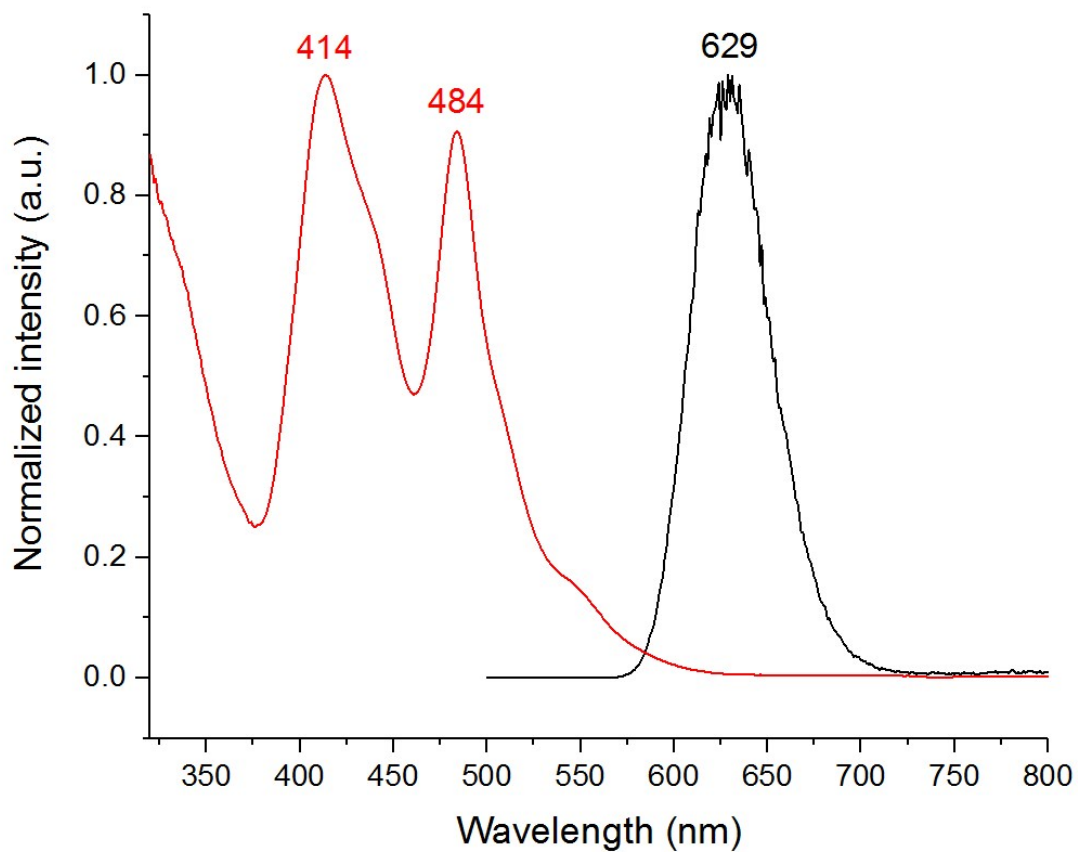**Figure S10.** Normalized absorption (red line) and emission (black line) spectra of **1b**.

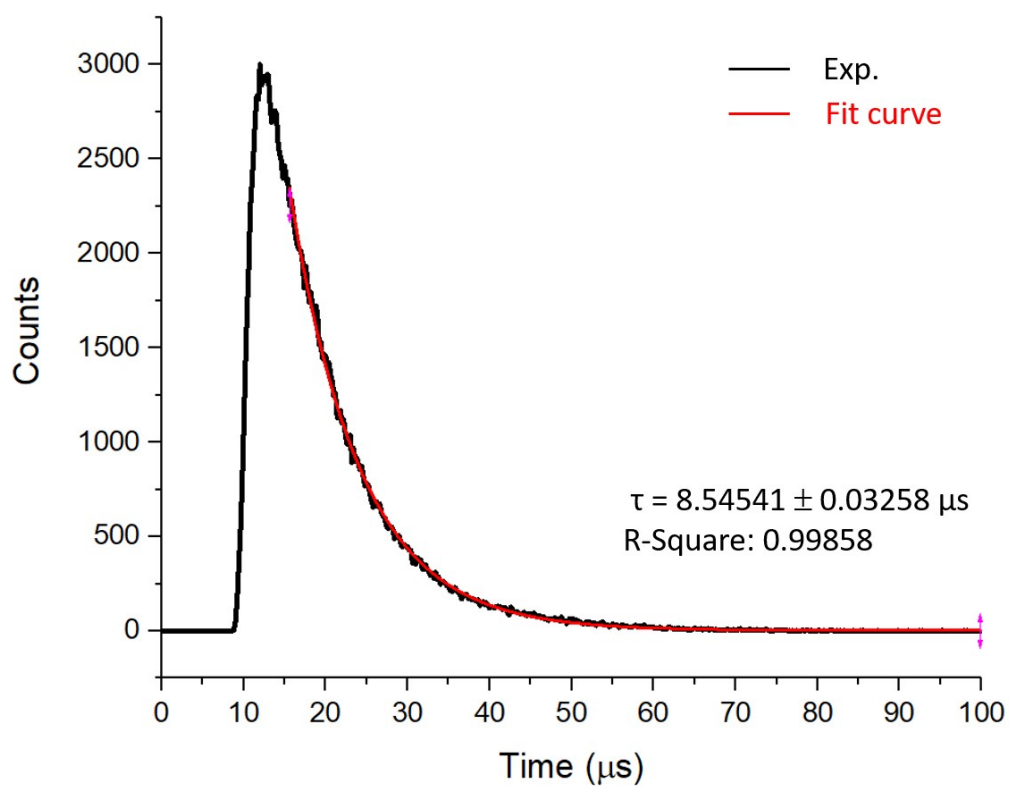**Figure S11.** Normalized absorption (red line) and emission (black line) spectra of **2**.

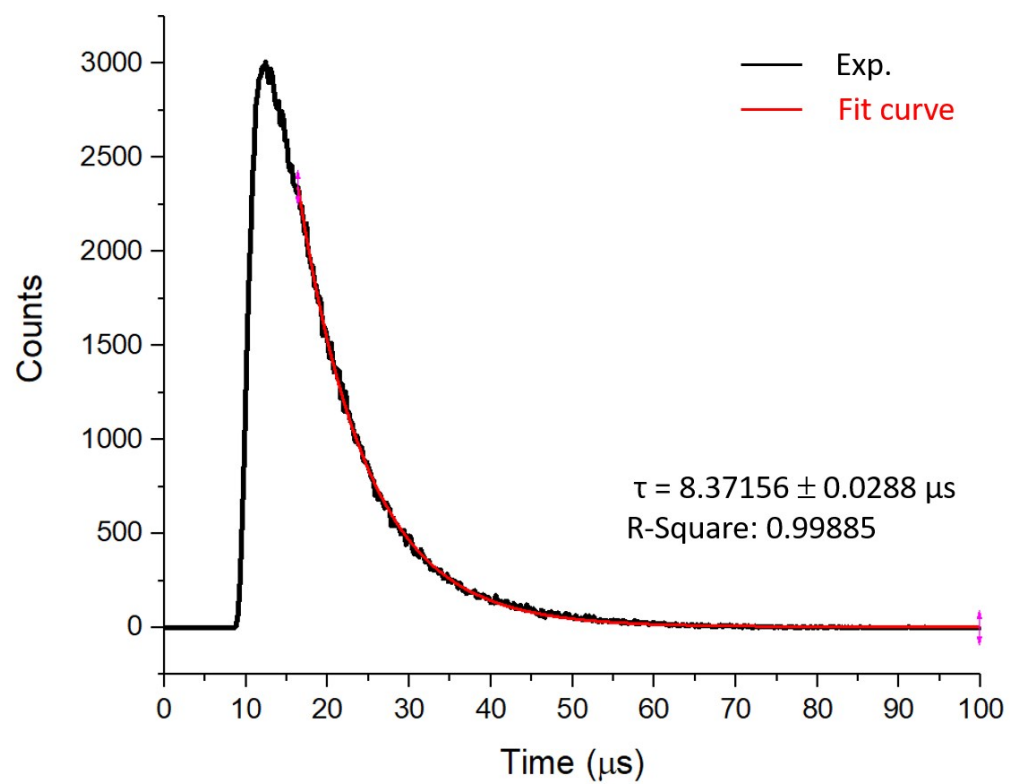**Figure S12.** Time-resolved photoluminescence spectrum of **1a**.

Figure S13. Time-resolved photoluminescence spectrum of **1b**.
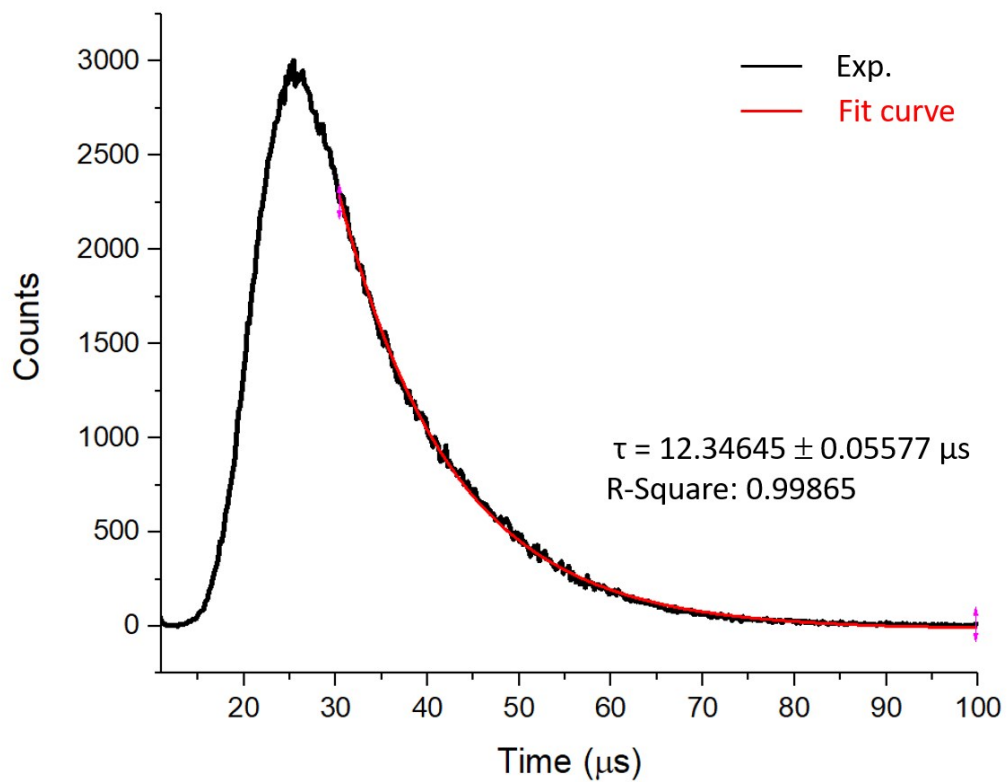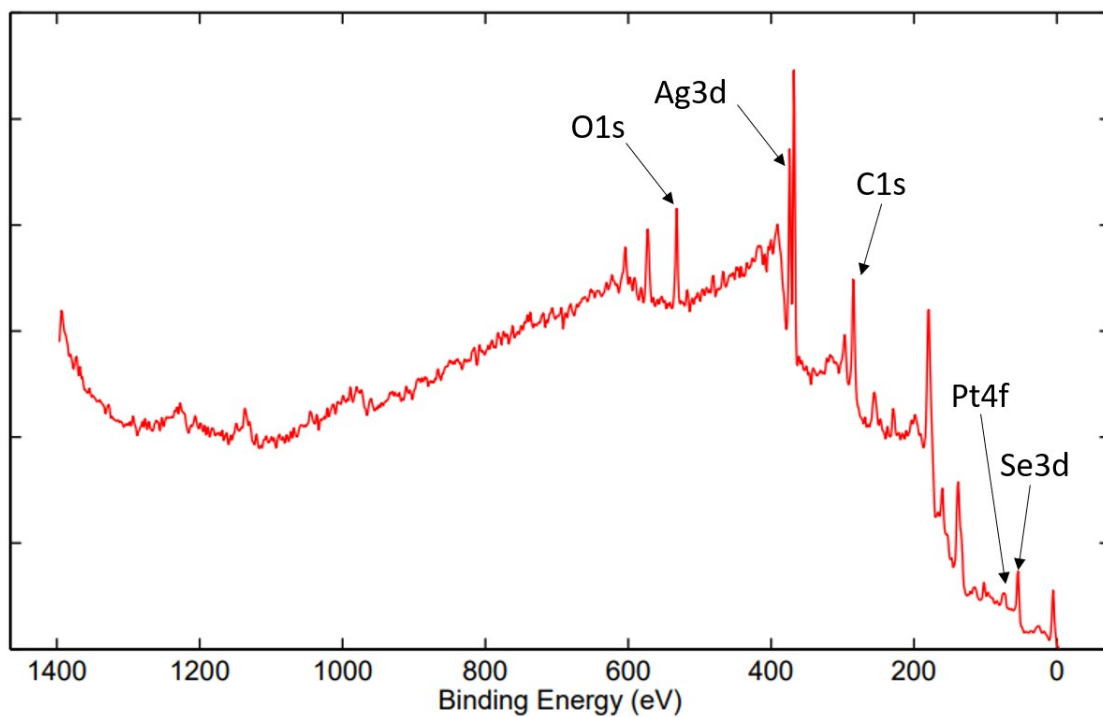
Figure S14. Time-resolved photoluminescence spectrum of **2**.

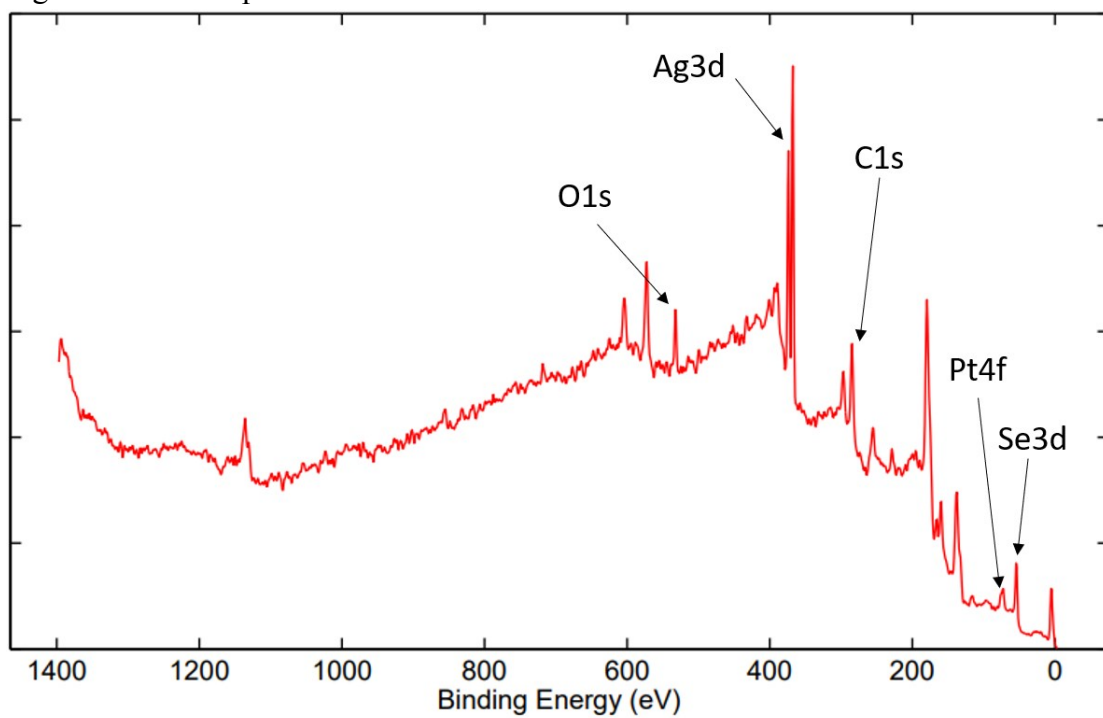Figure S15. XPS spectrum of **1a**.

Figure S16. XPS spectrum of **1b**.
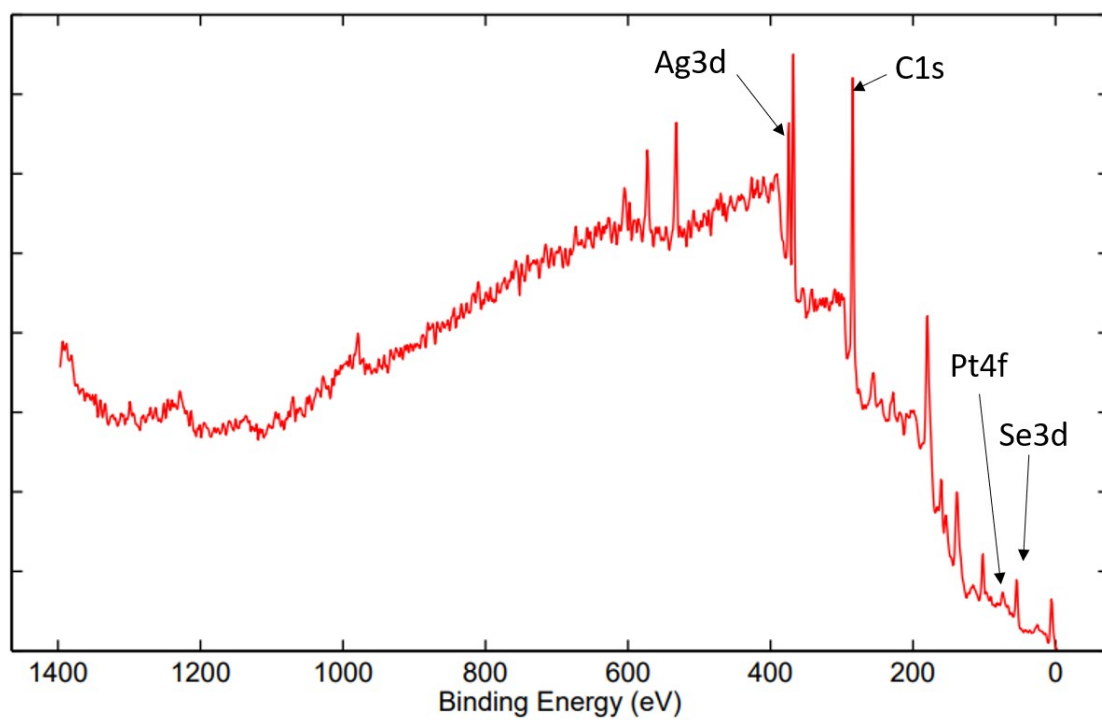
Figure **S17.** XPS spectrum of **2**.

Figure S18. (a) Ag 3d and (b) Pt 4f XPS spectrum of **1a**.

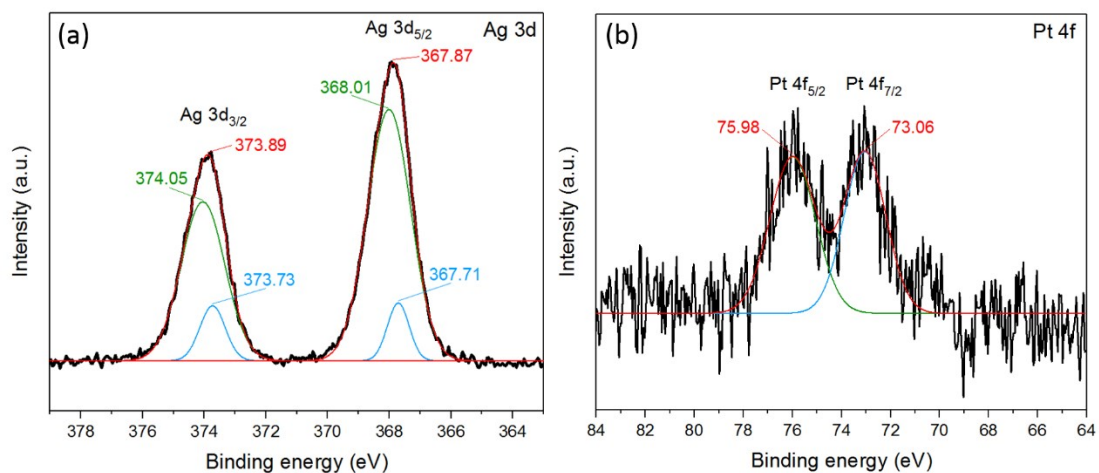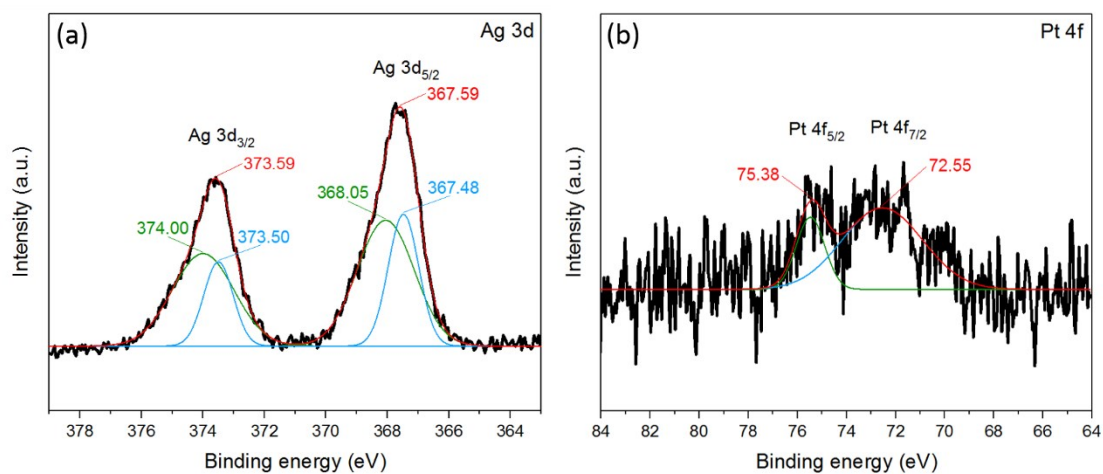**Figure S19.** (a) Ag 3d and (b) Pt 4f XPS spectrum of **1b**.
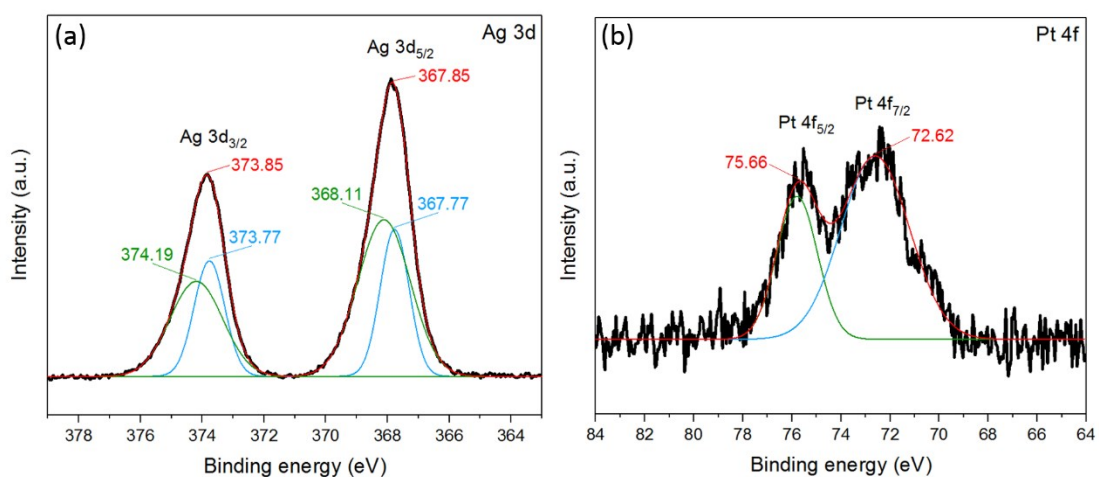

Figure S20. (a) Ag 3d and (b) Pt 4f XPS spectrum of **2**.

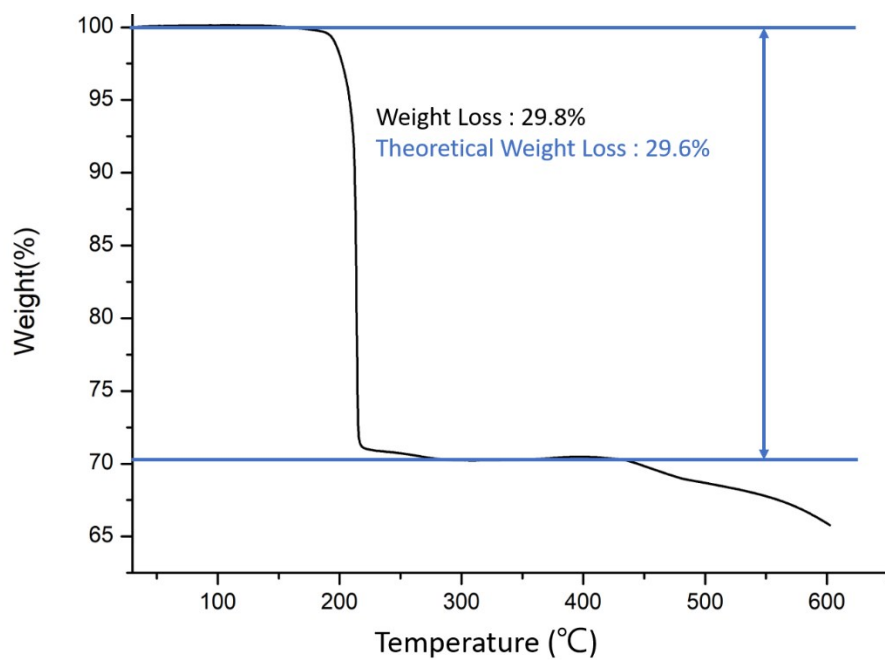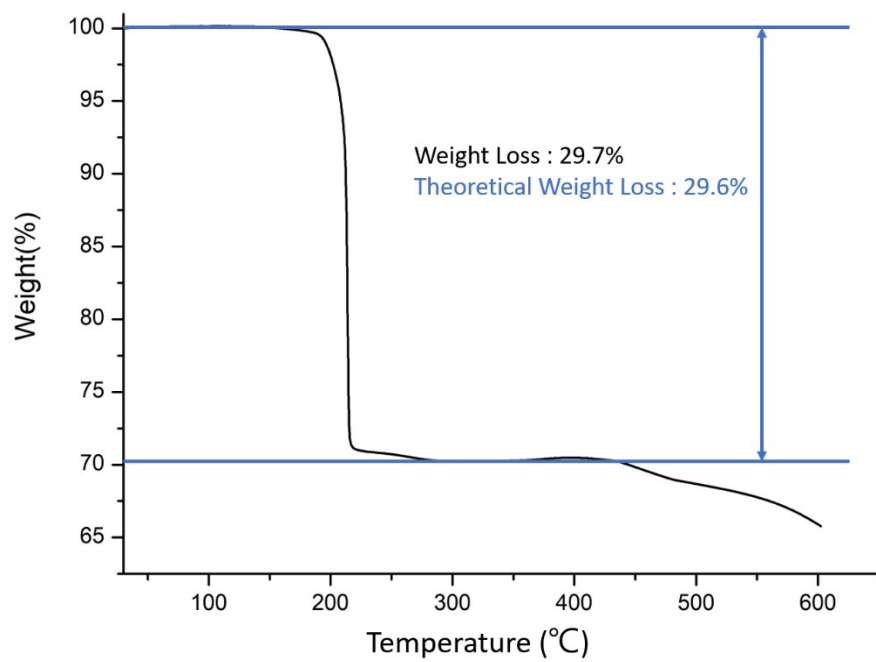**Figure S21.** TGA spectra of **1a.**
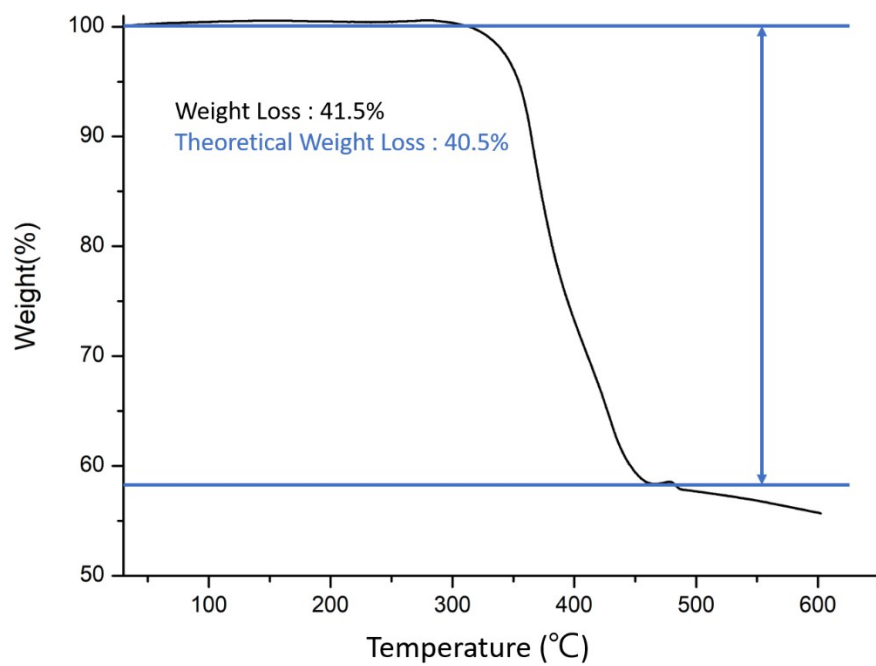

Figure S22. TGA spectra of **1b.**
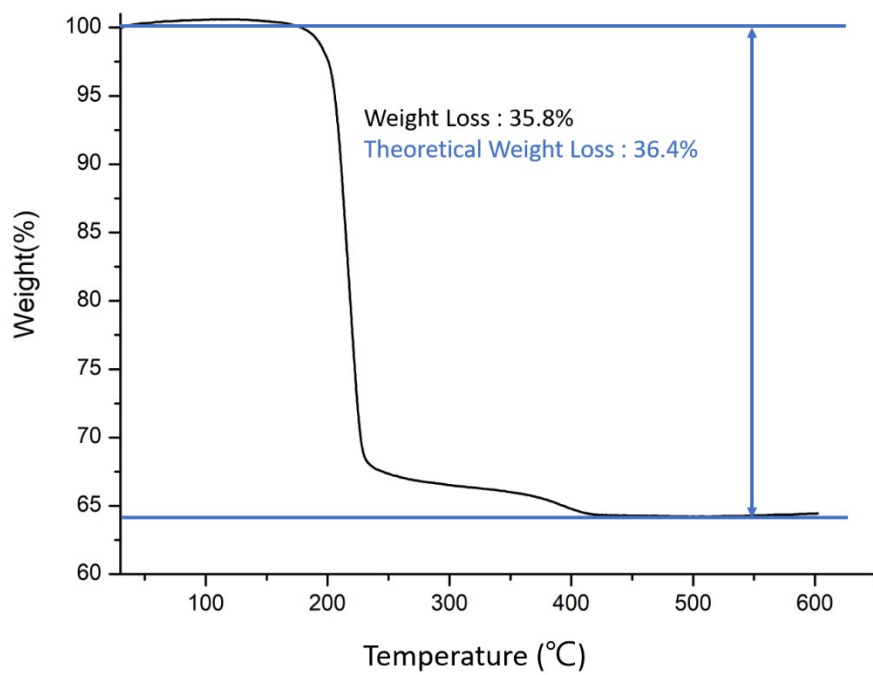
Figure S23. TGA spectra of **2.**

Figure S24. TGA spectra of **3.**
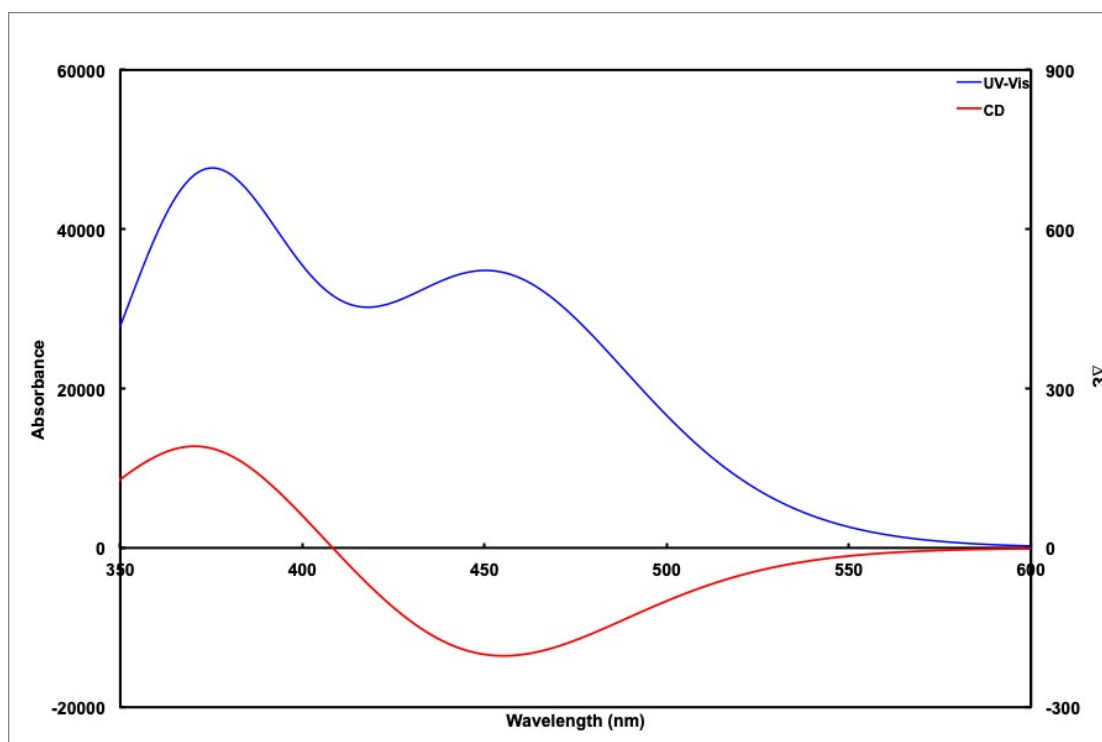
Figure S25. TD-DFT simulated UV-vis (blue) and CD (red) spectra of the **1'** model.

Table S1. Selected bond distances (Å) in **1a**, **1b** and **2**. The corresponding values for the DFT-optimized model **1'** of *T* structure, are also reported together with the corresponding averaged Wiberg indices into brackets.

	Pt-Ag$_{ico}$	Ag$_{ico}$-Ag$_{ico}$	Ag$_{ico}$-Ag$_{cap}$	Ag$_{ico}$-Se	Ag$_{cap}$-Se	Se...Se bite
1a	2.7428(12)- 2.7945(13) avg. 2.759(4)	2.8349(16)- 2.9556(16) avg. 2.901(9)	2.9130(20)- 3.0115(16) avg. 2.959(8)	2.6246(19)- 2.6910(20) avg. 2.658(7)	2.6010(20)- 2.6300(20) avg. 2.617(10)	3.664(2)- 3.707(2) avg. 3.688(2)
1b	2.7494(15)- 2.7601(14) avg. 2.756(4)	2.8349(16)- 2.9556(16) avg. 2.901(9)	2.9050(18)- 2.9956(19) avg. 2.949(9)	2.6600(20)- 2.6870(20) avg. 2.674(7)	2.6000(20)- 2.6450(20) avg. 2.621(10)	3.684(3)- 3.716(3) avg. 3.691(3)
2	2.7626(13)- 2.8232(15) avg. 2.791(5)	2.8484(17)- 3.2120(20) avg. 2.932(10)	2.9109(18)- 3.00490(20) avg. 2.975 (9)	2.6310(20)- 2.6760(20) avg. 2.651(7)	2.5730(20)- 2.6380(20) avg. 2.610(11)	3.643(3)- 3.701(3) avg. 3.665(3)
1' (DFT)	2.850 [0.155]	3.018-2.940 3.029 [0.085]	3.076-3.032 3.054 [0.038]	2.786 [0.164]	2.721-2.707 2.714 [0.223]	3.814

Table S2. Selected X-ray crystallographic data of **1a**, **1b** and **2**.

Compound	1a	1b	2
CCDC number	1985876	2069764	2069767
Empirical formula	$C_{72}H_{168}Ag_{20}O_{24}P_{12}PtSe_{24}$	$C_{72}H_{168}Ag_{20}O_{24}P_{12}PtSe_{24}$	$C_{192}H_{216}Ag_{20}P_{12}PtSe_{24}$
Crystal system, space group	Monoclinic, $P2_1$	Monoclinic, Pn	Triclinic, $P\overline{1}$
a, Å	15.9963(6)	17.9783(12)	18.4077(12)
b, Å	29.4039(11)	26.4928(18)	18.8892(13)
c, Å	16.5323(6)	18.7771(13)	33.160(2)
α, deg.	90	90	78.1000(10)
β, deg	107.5256(8)	112.7096(12)	84.0500(10)
γ, deg	90	90	83.2810(10)
Volume, Å^3	7415.1(5)	8250.1(10)	11167.1(13)
Z	2	2	2
ρ_{calcd}, g·cm^{-3}	2.704	2.500	2.124
μ, mm^{-1}	9.582	8.618	6.374
Temperature, K	150(2)	100(2)	150(2)
θ_{max}, deg. / completeness, %	25.00 / 99.9	25.00 / 99.6	24.99 / 98.6
Reflections collected / unique	42098 / 19437 [R(int) = 0.0340]	58143 / 27116 [R(int) = 0.0309]	64121 / 38771 [R(int) = 0.0483]
Restraints / parameters	462 / 1394	495 / 1576	2007 / 1567
R1[a], wR2[b] [I > 2σ(I)]	0.0380,0.0957	0.0367, 0.0943	0.0770,0.2120
R1[a], wR2[b] (all data)	0.0428,0.0989	0.0432, 0.0981	0.1390,0.2383
Absolute structure parameter	0.139(8)	0.293(7)	-
Goodness of fit on F^2	1.023	1.039	1.034
Largest diff. peak and hole, e/Å^3	2.391 and -1.609	2.517 and -1.146	3.973 and -2.658

[a]$R1 = \Sigma \mid \mid F_o \mid - \mid F_c \mid \mid / \Sigma \mid F_o \mid$. [b]$wR2 = \{ \Sigma[w(F_o^2 - F_c^2)^2] / \Sigma[w(F_o^2)_2] \}^{1/2}$

Reference

S1. D. D. Perrin, W. L. F. Armarego, *Purification of laboratory chemicals*. 3rd Edition, Pergamon Press, Oxford, 1988.

S2. T.-H. Chiu, J.-H. Liao, F. Gam I. Chantrenne, S.Kahlal, J.-Y. Saillard and C. W. Liu, *J. Am. Chem. Soc.*, 2019, **141**, 12957

S3. C. W. Liu, I.-J. Shang, C.-M. Hung, J.-C. Wang and T.-C. Keng, *J. Chem. Soc., Dalton Trans.* 2002, 1974.

S4. B. A. Trofimov, A. V. Artem'ev, S. F. Malysheva, N. K. Gusarova, *Dokl. Chem.*, 2009, **428**, 225-227.

S5. SADABS, version 2014-11.0, Bruker Area Detector Absorption Corrextions, Bruker AXS Inc., Madison, WI, 2014.

S6. SAINT, V8.30A, Software for the CCD detector system, Bruker Analytical: Madison, WI, 2012.

S7. G. M. Sheldrick, *Acta Cryst. A*, 2008, **64**, 112.

S8. SHELXTL, version 6.14, Bruker AXS Inc., Madison, Wisconsin, USA, 2003.

S9. Gaussian 16, Revision A.03, M. J. Frisch, G. W. Trucks, H. B. Schlegel, G. E. Scuseria, M. A. Robb, J. R. Cheeseman, G. Scalmani, V. Barone, G. A. Petersson, H. Nakatsuji, X. Li, M. Caricato, A. V. Marenich, J. Bloino, B. G. Janesko, R. Gomperts, B. Mennucci, H. P. Hratchian, J. V. Ortiz, A. F. Izmaylov, J. L. Sonnenberg, D. Williams-Young, F. Ding, F. Lipparini, F. Egidi, J. Goings, B. Peng, A. Petrone, T. Henderson, D. Ranasinghe, V. G. Zakrzewski, J. Gao, N. Rega, G. Zheng, W. Liang, M. Hada, M. Ehara, K. Toyota, R. Fukuda, J. Hasegawa, M. Ishida, T. Nakajima, Y. Honda, O. Kitao, H. Nakai, T. Vreven, K. Throssell, J. A. Montgomery, Jr., J. E. Peralta, F. Ogliaro, M. J. Bearpark, J. J. Heyd, E. N. Brothers, K. N. Kudin, V. N. Staroverov, T. A. Keith, R. Kobayashi, J. Normand, sK. Raghavachari, A. P. Rendell, J. C. Burant, S. S. Iyengar, J. Tomasi, M. Cossi, J. M. Millam, M. Klene, C. Adamo, R. Cammi, J. W. Ochterski, R. L. Martin, K. Morokuma, O. Farkas, J. B. Foresman, D. J. Fox, Gaussian, Inc., Wallingford CT, 2016.

S10. a) A. D. Becke, *Phys. Rev. A*, 1988, **38**, 3098-3100; b) J. P. Perdew, *Phys. Rev. B*, **33**, 8822-8824.

S11. a) A. Schaefer, H. Horn, R. Ahlrichs, *J. Chem. Phys.*, 1992, **97**, 2571-2577; b) A. Schaefer, C. Huber, R. Ahlrichs, *J. Chem. Phys.*, 1994, **100**, 5829-5835.

S12. E. D. Glendening, J. K. Badenhoop, A. E. Reed, J. E. Carpenter, J. A. Bohmann, C. M. Morales, C. R. Landis, F. Weinhold, *NBO 6.0*; Theoretical Chemistry Institute, University of Wisconsin, Madison, WI, 2013, http://nbo6.chem.wisc.edu.

S13. a) T. H. Dunning Jr. and P. J. Hay, (Eds. H. F. Schaeffer), Plenum Press: New

York, 1977; b) P. J. Hay and W. R. Wadt, *J. Chem. Phys*., 1985, **82**, 270-283; c) P. J. Hay, W. R. Wadt, *J. Chem. Phys.,* 1985, **82**, 284-298; d) P. J. Hay, W. R. Wadt, *J. Chem. Phys*., 1985, **82**, 299-310; e) A, Schafer, H. Horn, R. Ahlrichs, *J. Chem. Phys*., 1992, **97**, 2571-2577.

S14. T. Yanai, D. Tew, N. Handy, *Chem*. *Phys. Lett*., 2004, **393**, 51-57.

S15. S. I. Gorelsky, SWizard program, revision 4.5, http://www.sg-chem.net.

S16. S. I. Gorelsky, AOMix program, http://www.sg-chem.net.